Coherent optical imaging and guided interventions in breast cancer: translating technology into clinical applications

Stephen Boppart, Freddy Nguyen, Adam Zysk, Eric Chaney, Jan Kotynek, et al.

Stephen A. Boppart M.D., Freddy T. Nguyen, Adam M. Zysk, Eric J. Chaney, Jan G. Kotynek, Uretz J. Oliphant, Frank J. Bellafiore, Kendrith M. Rowland, Patricia A. Johnson, "Coherent optical imaging and guided interventions in breast cancer: translating technology into clinical applications," Proc. SPIE 6991, Biophotonics: Photonic Solutions for Better Health Care, 699102 (17 April 2008); doi: 10.1117/12.780168

SPIE.

Event: SPIE Photonics Europe, 2008, Strasbourg, France

Coherent Optical Imaging and Guided Interventions in Breast Cancer: Translating Technology into Clinical Applications

Stephen A. Boppart[*,a-d,f-h], Freddy T. Nguyen[a,b,e-g], Adam M. Zysk[a-c,g], Eric J. Chaney[a,b,g], Jan G. Kotynek[f-h], Uretz J. Oliphant[f-h], Frank J. Bellafiore[f-h], Kendrith M. Rowland[f-h], Patricia A. Johnson[f-h]

[a]Biophotonics Imaging Laboratory, [b]Beckman Institute for Advance Science and Technology, [c]Department of Electrical and Computer Engineering, [d]Department of Bioengineering, [e]Department of Chemistry, Medical Scholars Program, [f]College of Medicine, [g]University of Illinois at Urbana-Champaign, 405 North Mathews Avenue, Urbana, IL, USA 61801; [h]Mills Breast Cancer Institute, Carle Foundation Hospital, Carle Clinic Association, 611 West Park Street, Urbana, IL, USA 61801

*boppart@uiuc.edu; http://www.biophotonics.uiuc.edu/

ABSTRACT

Breast cancer continues to be one of the most widely diagnosed forms of cancer in women and the second leading type of cancer deaths for women. The metastatic spread and staging of breast cancer is typically evaluated through the nodal assessment of the regional lymphatic system, and often this is performed during the surgical resection of the tumor mass. The recurrence rate of breast cancer is highly dependent on several factors including the complete removal of the primary tumor during surgery, and the presence of cancer cells in involved lymph nodes. Hence, developing means to more accurately resect tumor cells, along with the tumor mass, and ensure negative surgical margins, offers the potential to impact outcomes of breast cancer. The use of diffuse optical tomography has been applied for screening optical mammography applications as an alternative to standard x-ray mammography. The use of coherence ranging and coherent optical imaging in breast tissue has also found numerous applications, including intra-operative assessment of tumor margin status during lumpectomy procedures, assessment of lymph node changes for staging metastatic spread, and for guiding needle-biopsy procedures. The development, pre-clinical testing, and translation of techniques such as low-coherence interferometry (LCI) and optical coherence tomography (OCT) into clinical applications in breast cancer is demonstrated in these feasibility studies.

Keywords: Optical Coherence Tomography, Breast Cancer, Metastasis, Clinical Imaging, Lymph Node, Biomedical Optics, Image Guided Surgery.

1. INTRODUCTION

1.1 Breast Cancer

Breast cancer continues to have a significant impact on the lives of individuals throughout the world. According to recent U.S. cancer statistics, an estimated 178,480 new cases of invasive breast cancer and approximately 62,030 new cases of *in situ* breast cancer are expected to occur this year, making it the most frequently diagnosed non-skin cancer in U.S. women [1]. Breast cancer ranks second among cancer deaths in women in the U.S., with an estimated 40,910 deaths anticipated in 2007. In a woman's lifetime the probability of developing invasive breast cancer is now 1 in 8. Early detection and treatment has resulted in a more favorable prognosis. The 5-year relative survival rate for localized breast cancer in the U.S. is now close to 100%, compared to only 72% in the 1940s [2]. After 5 years, survival following the diagnosis of breast cancer continues to fall for all stages. This data indicates that current detection methods and treatment protocols must still be improved.

As of January 2002, the U.S. National Cancer Institute estimated that 2.3 million women have had a history of breast cancer, which points to the importance in monitoring for the recurrence of this disease. Being able to detect smaller foci of cancer cells as well as being able to detect other progressive changes in not only the tissue morphology but also the molecular make-up of the tissue will provide further insights into how to not only better diagnose but also better treat

Biophotonics: Photonic Solutions for Better Health Care, edited by
Jürgen Popp, Wolfgang Drexler, Valery V. Tuchin, Dennis L. Matthews,
Proc. of SPIE Vol. 6991, 699102, (2008) · 1605-7422/08/$18 · doi: 10.1117/12.780168

earlier stages of breast cancer. There is a continued emphasis on the early diagnosis of breast cancer in order to provide better managed care, and across all clinical imaging modalities, there are advances in our ability to detect smaller and smaller lesions, striving toward the detection of changes at the molecular and cellular levels.

The ability to detect and remove all of the tumor present at these very early stages, including small nests or foci of tumor cells, and especially prior to cellular metastases, is essential for lowering the breast cancer mortality rate. As the detection of smaller, early-stage cancers and any metastases becomes more common, advanced technologies with the capabilities to detect, identify, and guide the removal of these small lesions and metastases will be needed. While breast cancer represents one clinical disease where high-resolution surgical guidance will become necessary, this is only representative of a large number of other clinical scenarios, such as in the surgical treatment of other solid tumors of the brain, lung, liver, and bladder, to name only a few.

1.2 Surgical Margin Assessment

A current challenge in the surgical treatment of breast cancer is the complete surgical resection of tumor masses during breast conserving procedures, such as lumpectomies. While it is relatively straightforward to resect the bulk of tumors identified on mammography, it is common to take wide surgical margins in an effort to remove small foci of tumor cells that may have extended beyond the central tumor. Very often, techniques such as frozen-section pathology or touch-prep technologies are used during a surgical operation to provide a level of microscopic assessment or analysis of the tumor margin for the presence of tumor cells [3,4]. Unfortunately, many have challenged the usefulness of these procedures because of potentially limited prognostic value in the results [3,5,6]. A major limitation to pathology, either intra-operatively or post-operatively, is that a significant degree of under-sampling of the surgical margin occurs. Often, due to limitations of cost and time, a limited set (~10) of histological sections are sampled, selected by visual assessment of suspicious regions. This, however, represents a drastically small area of coverage or sampling, compared to the entire surgical margin surface. For a 10 cm resected tissue mass, examining 10 histological sections from the surgical margin represents less than 0.002% of the surgical margin surface area. What is needed, therefore, is a means for rapidly assessing surgical margins intra-operatively, covering large areas with micron-scale resolution.

The feasibility of using OCT to image tumor margins for breast cancer was first demonstrated in an NMU-carcinogen induced rat mammary model [7], and recent reports have investigated the optical properties of normal and neoplastic breast tissue using various LCI or OCT techniques [8-11]. Studies have translated portable OCT technology into clinical and surgical applications, with intra-operative imaging being demonstrated [12,13].

1.3 Lymph Node Assessment

The staging of breast cancer is currently based on three main criteria: the size of the primary tumor, the infiltration of lymph nodes by cancer cells, and the subsequent metastasis of cancer cells to other sites. Table 1 delineates the current criteria used by U.S. physicians to stage the progression of breast cancer in patients [14]. The status of lymph node involvement has long been used by the medical community for determining the metastatic state of the cancer. The metastatic spread of cancer from the primary tumor to a secondary site is a process that is typically preceded by the migration of tumor cells via the lymphatic or vascular circulatory systems. The tumor cells that have detached themselves from the primary tumor must invade through the basement membrane and into the lymphatic or vascular circulatory systems. Once in the lymphatic system, free tumor cells are shuttled through the lymph vessels to the lymph nodes where they either are recognized, processed, and destroyed by the immune system, or they are capable of evading or overwhelming the immune system.

The ability to identify the migration of cancer cells away from the primary tumor using pre-operative or intra-operative imaging techniques is currently and active area under investigation. The 5-year survival rate for U.S. breast cancer patients (Table 2) when the disease is detected at a localized stage is currently 100% [15]. However, according to the American Cancer Society statistics, approximately 36.3% of the newly reported breast cancer cases in the U.S. are diagnosed at later stages when the tumor is no longer localized [15]. These data obviously suggest that the earlier breast cancer can be detected, the more amenable is it to be treated, and cured.

Table 1. Staging of breast cancer [14].

Staging Breast Cancer			
Stage	Tumor Size	Lymph Node Involvement	Metastasis
I	< 2cm	No	No
II	2-5 cm	No/Ipsilateral	No
III	> 5cm	Yes/Ipsilateral	No
IV	N/A	N/A	Yes

Table 2. Five-year survival rate dependent on stage of breast cancer (U.S. American College of Surgeons National Cancer Data Base, for patients diagnosed from 1995-1998).

Survival Rates	
Stage	5-Year Survival Rate
0	100%
I	100%
IIA	92%
IIB	81%
IIIA	67%
IIIB	54%
IV	20%

As has been previously demonstrated, OCT can be used to visualize the microstructure of lymph nodes such as the capsule, the follicles, and the sinuses located within the cortex of the lymph nodes [16]. These preliminary experiments indicate that OCT could potentially be used to perform intra-operative *in vivo* nodal assessment [17]. By providing real-time assessment of the lymph nodes, surgeons would be able to reduce the amount of non-diagnostic tissue removed during surgery. In addition, reducing the number of nodes during surgery will decrease the chances of developing lymphedema. Currently 20% - 30% of patients who have had their axillary lymph nodes removed develop lymphedema [18]. Lymphedema is the accumulation of lymph in the interstitial spaces due to the disruption of the lymphatic system by the removal of lymph nodes. Risk factors of lymphedema include nodal dissection of the axillary lymph nodes, radiation therapy in the treatment of breast cancer, and the presence of cancer cells in the resected lymph nodes. For these patients, pathology reports indicated the vast majority of the lymph nodes removed do not contain any tumor cell deposits within the lymph nodes (< 5%). This small number in lymph node involvement is more likely due to the recent advancements in early breast cancer screening and diagnosis, allowing physicians and surgeons to treat patients at earlier stages, and leading to a higher survival rate from breast cancer.

1.4 Needle-Biopsy Guidance

Prior to most breast cancer related surgical procedures such as excisional breast biopsy, lumpectomy, or mastectomy, fine-needle or core-needle biopsies are acquired from the mass to acquire cells and tissue to make a pathological diagnosis. Guiding techniques, such as ultrasound imaging or x-ray stereotactic imaging, have experienced sampling difficulties, primarily because of imaging resolution and a disconnect between the imaging projections and planes and the needle-tip position in 3-D space, deep within breast tissue. The incorporation of fiber-based OCT beam delivery into a biopsy needle would provide real-time information for guiding the needle to the appropriate location of the breast lesion for biopsies or for the placement of wire localization [10,19-21]. Studies have shown that there is diagnostically significant information within the backscattering signals and the refractive index data that can be used to differentiate

between various tissue types found in breast lesions. There are also reported studies that have examined the spectral information from single axial scan lines [8]. Using newly developed computational algorithms, one can analyze the spatial frequency content or periodicity of the axial scan data to distinguish between normal tissue and invasive ductal carcinoma lesions with high sensitivity [8,21]. Due to the deep location of many breast lesions, the use of needle-based imaging probes will be needed to place the suspicious breast lesion within the working distance of the OCT beam.

2. METHODOLOGY

2.1 Instrumentation (hardware)

The portable clinical OCT system (Fig. 1) developed for these translational investigations is a spectral domain OCT (SD-OCT) system which uses light from a superluminescent diode (BWTek–SLD1C) centered at 1310 nm with a bandwidth of 92 nm. The source is coupled into a low-loss optical circulator (Gould Fiber Optics – CIRC-3-31-P-BB-10-6: 3 port) which helps maintain the power of the signal coming back from the fiber coupler to the detector. From the circulator, the light is passed into a 95/5 fiber optic splitter (Gould Fiber Optics, Inc.) which splits the incident light into the sample and reference arms of the interferometer. The sample arm currently uses a 60 mm achromatic lens focusing approximately 4.75 mW of light onto a 35.0 µm spot size (transverse resolution). The broad bandwidth of the laser source yields an axial resolution of approximately 8.3 µm in free space or 5.9 µm in tissue, assuming an average index of 1.4. The objective lens in the sample arm was chosen to roughly match its confocal parameter (1.47 mm) to the penetration depth (2 mm) observed in imaging human breast cancer samples. The light reflected back from the mirror in the reference arm and the tissue specimen in the sample arm are re-coupled through the two arms of fiber optic splitter and a set of polarizer controllers (Fiber Control: FPC-2). Through the fiber coupler, a commonly-used Michelson-type interferometer couples the beams of light from the two arms, the reference and sample arms. The resulting OCT signal is subsequently passed through the optical circulator and into the detector arm. Spatial scanning in the X-Y plane is currently performed by a set of galvanometers with a telecentric probe to scan the beam across the sample surface. Data acquisition is achieved via a spectrometer setup which collimates the OCT beam onto a plane ruled reflectance grating (Richardson Gratings, Newport Corporation, 53004BK01-148R). The diffraction grating with 1000 grooves/mm and blazed for 1310 nm is used to disperse the light which is focused by a 150 mm singlet lens onto an InGaAs line scan camera (Sensors Unlimited SU1024LE-1.7T1-0500) with 1024 pixels. The data acquisition is accomplished through a National Instruments NI-DAQ card (#PCI-6111E) in a dual Xeon processor (3.20 GHz) computer with 1 GB RAM. With exposure times ranging from 24.4 µs to 408.4 µs, the measured SNR ranges from 96 dB to 116 dB respectively

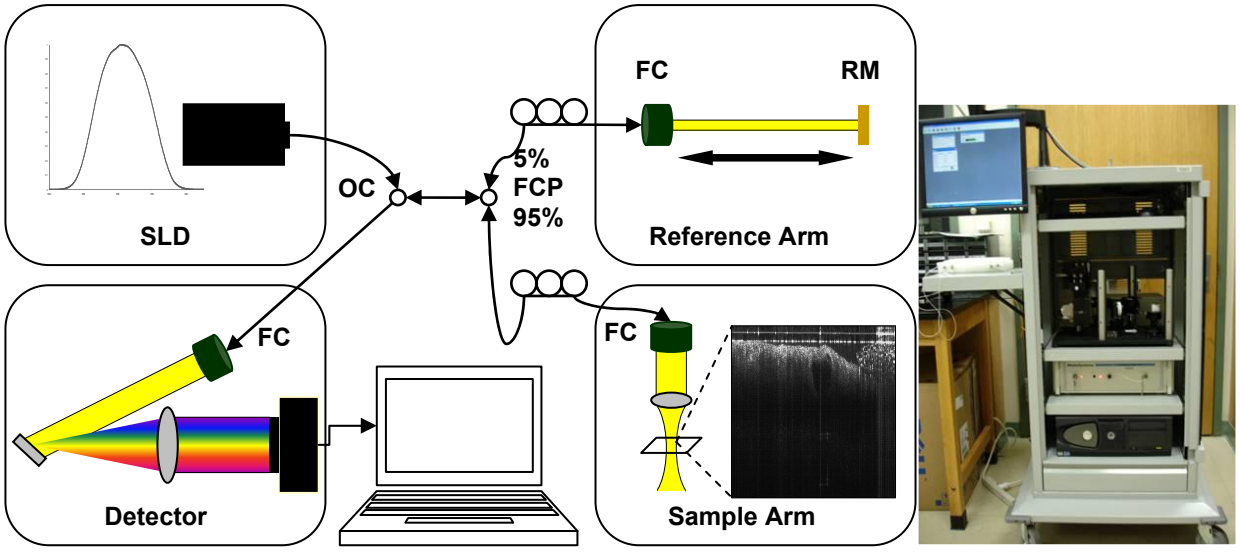

Fig. 1. Schematic diagram and photograph of the clinical spectral-domain optical coherence tomography system. OC – Optical Circulator, FC – Fiber Collimator, FCP5/95 – Fiber Coupler, RM – Reference Mirror.

2.2 Instrumentation (software)

The OCT instrument is controlled by a custom LabVIEW software package which interacts directly with the galvanometers and the line scan camera. It also interfaces with a data processing sequence written in Matlab/C++. The raw signal received from the line scan camera is first up-sampled through zero-padding in the time domain. Due to the non-linear response in the grating, line scan camera, and other optics in the system, a cubic spline interpolation was implemented to compensate for these aberrations. The spline interpolation parameters are calculated using collected data from a perfect reflector placed at the focus of the sample arm while the reference arm is translated, moving the corresponding signal throughout different depths of the OCT image. The collected data is compiled to yield a Modulation Transfer Function (MTF). The spline interpolation parameters are optimized to give the flattest MTF possible. These parameters are determined each time the detector arm of the system is realigned. The up-sampled data is re-indexed in the frequency domain using the spline interpolation. Lastly, a Fourier Transform is performed to transform the data from the spectral domain to the time domain, producing the OCT image.

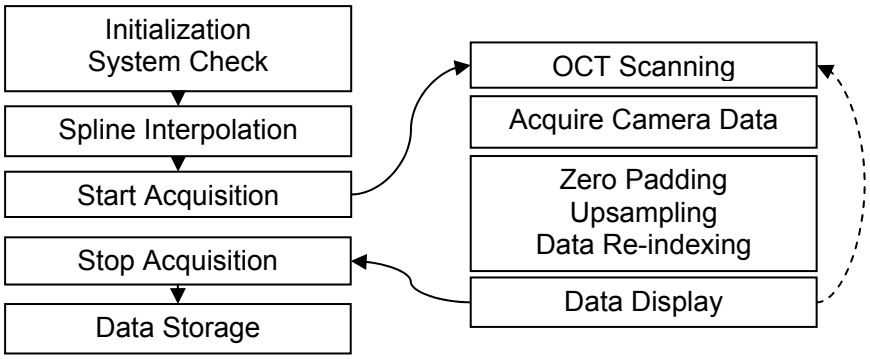

Fig. 2. Flow diagram for the acquisition software indicating the major components and processes.

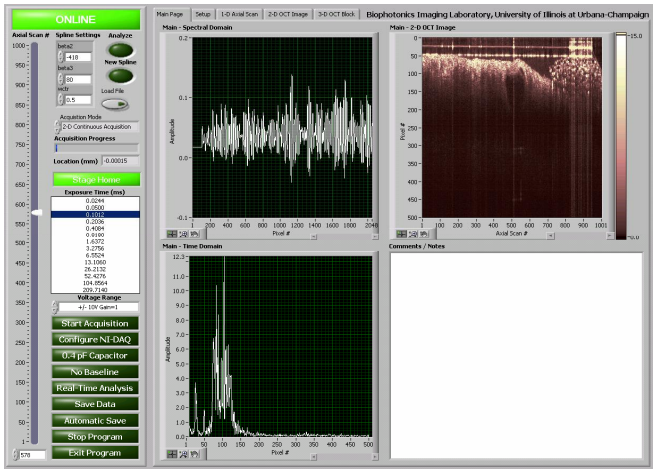

Fig. 3. Graphical User Interface with main overview screen containing raw signal (upper left), depth-dependent axial scan (lower left), and OCT cross-sectional image (upper right). The space in the lower right is reserved for comments on the imaging session and specimen.

2.3 Human subjects protocol

The recruitment and enrollment of patients was performed by clinical collaborators from Mills Breast Cancer Institute, Carle Foundation Hospital, and Carle Clinic Association, Urbana, Illinois, USA, who identified potential human subjects based on patients scheduled to undergo lumpectomy procedures for the removal of primary tumors diagnosed as ductal carcinoma *in situ* (DCIS) or invasive carcinoma of the breast. The patients were included in this study if their lesions were greater than 1 cm in size, diagnosed on needle-biopsy, and in need of surgical resection, as determined by the physician based on medical histology, previous radiological films, and/or other relevant diagnostic results. All

recruitment and research protocols were approved by the Institutional Review Boards of the University of Illinois at Urbana-Champaign and Carle Foundation Hospital. Potential subjects were informed about the study, the procedures, and the potential benefits and risks, and were consented prior to the surgery in accordance with the approved IRB protocols. To date over 20 patients have been enrolled in the study where tissue specimens were imaged at the Beckman Institute, and over 60 patients have been enrolled in the second study for real-time imaging in the operating room using the clinical OCT system.

2.4 Imaging protocols

The clinical OCT system was initially tested using the same human breast cancer specimen imaged under the Clinical SD-OCT system (1310 nm CW, 92 nm BW, 116 dB SNR, 5,000 lines/sec acquisition rate), a titanium:sapphire-based Time Domain OCT (TD-OCT) system (800 nm CW, 120 nm BW, 106 dB SNR, 10 lines/sec acquisition rate), and a titanium:sapphire-based SD-OCT system (800 nm CW, 120 nm BW, 96 dB SNR, 29,000 lines/sec acquisition rate). The 800 nm OCT systems were also used in ongoing studies of human cancer specimens received from Carle Foundation Hospital. These specimens were excess tissue discarded by the pathology department during examination and diagnosis of the tissue received from lumpectomy or mastectomy procedures. The specimens were transported to the Beckman Institute for Advanced Science and Technology where 3-D OCT images were taken along the tumor margins and the tissues were fixed and stained with haematoxylin and eosin (H&E).

At Carle Foundation Hospital, the clinical SD-OCT system was placed inside the operating room during lumpectomy procedures. After the tissue was removed from the patient but prior to being sent to the pathologist for gross examination and histological processing, the tissue specimens were imaged using the clinical OCT system. For surgical margin assessment, the OCT beam was scanned over a 1.0 cm x 1.0 cm region over areas that initially appear suspicious under visual examination. For optical needle-biopsy imaging and data collection, optical needle probes were inserted along or near the metal localization wire, if available, which was previously inserted under stereotactic x-ray guidance to guide the surgeon to the location of the tumor. After OCT imaging and data collection was completed, the tissue was inked to mark the location of the OCT scanning. The tissue was transported to the pathology department for gross examination of margins, and subsequently for sectioning and staining to provide correlation histology to the OCT images. A subset of the patients also had their lymph nodes removed as per standard of care, and these were imaged with OCT to assess for evidence of metastatic involvement. Resected lymph nodes were imaged intact, through the exposed capsule of the lymph nodes.

3. RESULTS

3.1 System validation

To initially evaluate OCT for the study of tumor margins, discarded excised tissue of a specimen with a tumor margin was imaged under the three OCT systems described in Section 2.4. These images (below and on following page) show that despite system differences, there are still observable similarities in detectable tissue features, along with reasonable penetration depths for breast tissue.

(a) 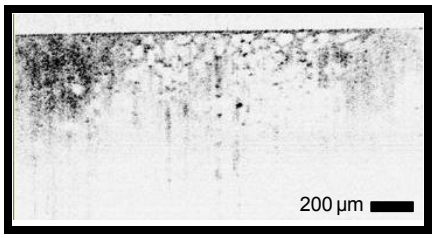

(b) 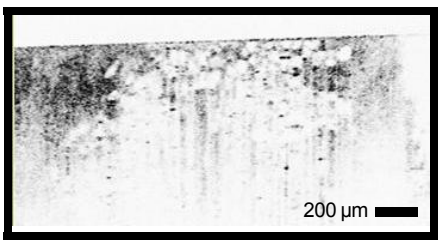

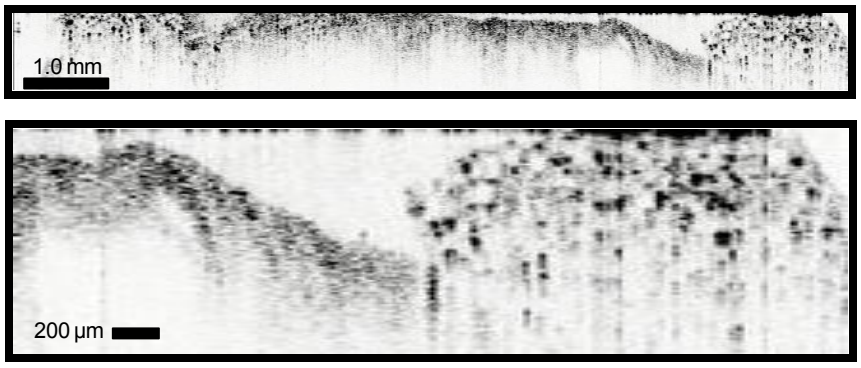

Fig. 4. OCT images of the same tissue specimen taken with three different OCT systems. On visual examination, the left portions of the images (a) and (b) are of a tumor and the middle areas are adipose cells. Image (a) was taken with the TD-OCT system at 800 nm, and the image (b) was taken with the SD-OCT system at 800 nm. These images are both 2.0 x 1.0 mm. Image (c) was acquired with the SD-OCT system at 1300 nm wavelength, and was of the same tissue in (a) and (b) but in a plane parallel to those images. Image (d) is a magnified region of (c) near the tumor/adipose boundary.

3.2 Representative intra-operative surgical margin data

OCT evaluation of surgical margins was investigated in these studies. The surgical margin is defined to be the margin of the tissue that makes up the outer surface of the excised tissue. For an invasive primary tumor, the current standard of care calls for having at least a 1.0 cm margin of normal tissue around the primary tumor. Following resection, the assessment by the surgeon and the pathologist is made grossly to determine whether this 1 cm margin of tissue has been achieved. The surgical margin is defined to be the outer-most section of tissue compared to the tumor margin which is being defined as the margin separating the normal tissue from the primary tumor. However, there is no current method for the surgeon to define the microscopic margins in real-time during surgery. Pathologists will often perform frozen-section histology of the tissue in order to determine the microscopic margin status at the time of surgery, but this can be time consuming, imprecise, and often with little prognostic value. These steps are always followed post-operatively by traditional methods of tissue fixation, sectioning of the paraffin embedded tissue, and subsequent staining. The microscopic margin is synonymous with the surgical margin and is used interchangeably depending on whether one is examining the tissue through gross examination or through histology slides. A positive surgical margin is currently being defined as one where cancer cells are found along the surgical margin, typically within 1 mm of the resected tissue surface.

Presented below are sets of OCT images and corresponding histology taken from representative surgical margins which include normal adipose tissue (Fig. 5) and high-scattering, heterogeneously-appearing regions indicative of tumor cells (Fig. 6).

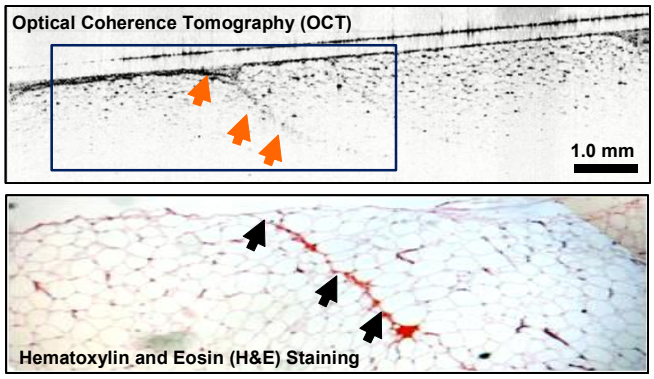

Fig. 5. OCT image (top) and corresponding histology (bottom) taken of the surgical margin of an excised tissue using the clinical SD-OCT at 1300 nm. The OCT image size is 10 x 3 mm. This image is mostly composed of adipose tissue. Arrows indicate a vascular structure within the adipose tissue.

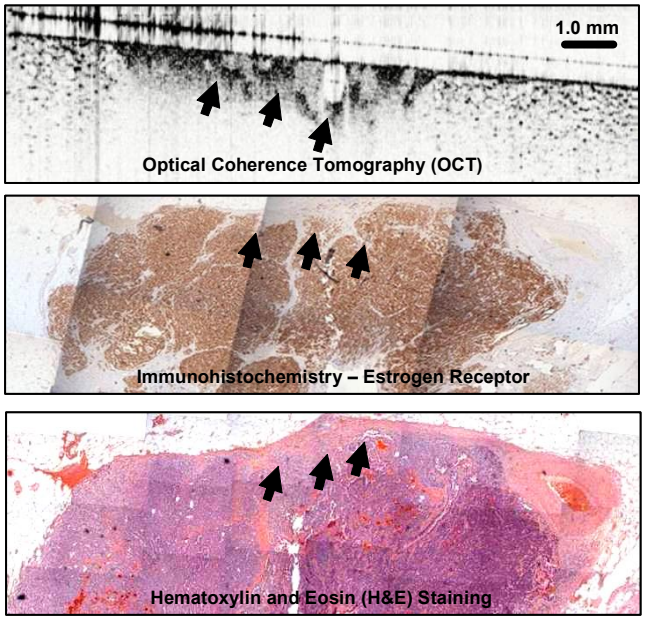

Fig. 6. OCT image (top) and corresponding histological tissue sections (middle, bottom) taken from the surgical margin of an excised tissue using the clinical SD-OCT at 1300 nm. The OCT image size is 10 x 3 mm. This image is composed of adipose tissue with a heterogeneous region of highly-scattering cells and structures (arrows). Histological findings of sections stained immunohistochemically for the estrogen receptor (middle) and with H&E (bottom) confirmed the presence of an invasive papillary carcinoma at the surgical margin.

Typically, the presence of tumor and tumor cells at the surgical margin is identified by regions of increased, heterogeneous scattering signals, as opposed to the lower-scattering signals from normal adipocytes. The highly-scattering areas of tumor can be differentiated from other scattering tissue artifacts, such as blood, which can be flushed or washed away, or coagulated tissue, which does not extend deep from the surgical margin. Ongoing studies are investigating how to further differentiate tumor tissue from connective stromal tissue, and determining the sensitivity and specificity of OCT tumor margin assessment compared to the gold standard of post-operative histology examination.

3.3 Representative intra-operative lymph node data

As previously mentioned, nodal assessment is a routine procedure that accompanies lumpectomies and mastectomies in order to stage the progression of the breast cancer. Representative 3-D OCT images of excised lymph nodes are shown in Fig. 7, along with corresponding histology. These specimens were imaged with our laboratory-based OCT system, where 3-D imaging was practical. Results show that the cortex regions of normal lymph nodes appears relatively homogeneous and lower in optical scattering, compared to the lymph nodes exhibiting metastatic cell involvement. During preliminary intra-operative imaging studies, resected lymph nodes from patients undergoing removal of axillary lymph nodes were imaged with OCT. These results are shown in Fig. 8.

The morphological features detected intra-operatively with OCT include the capsule surrounding the lymph nodes as well as scattering features several hundred microns into the cortex, such as within the follicular structures of the lymph nodes. Previous *ex vivo* OCT imaging has shown that optical scattering properties change within the cortex and the follicles [16], and scattering and size changes are likely to be detectable during real-time imaging. Ongoing studies are correlating intra-operative OCT image features with corresponding histological observations, as well as assessing the potential for detecting small micrometastases (< 2 mm foci) of tumor cells.

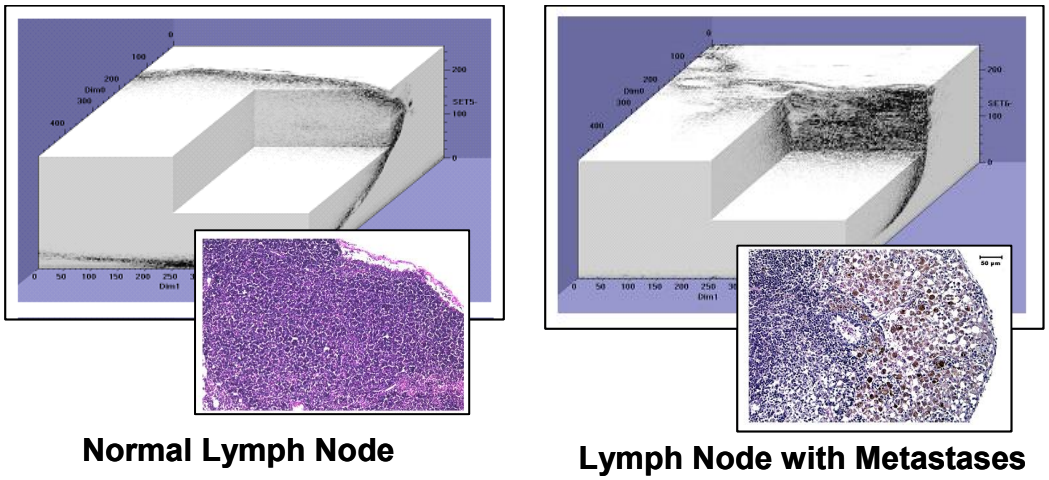

Fig. 7. Three-dimensional OCT images with cut-away views and corresponding histology acquired from resected human lymph nodes using our laboratory-based OCT system. Note the changes in the lymph node architecture due to the presence of the tumor cells results in an increase in the optical scattering detected with OCT.

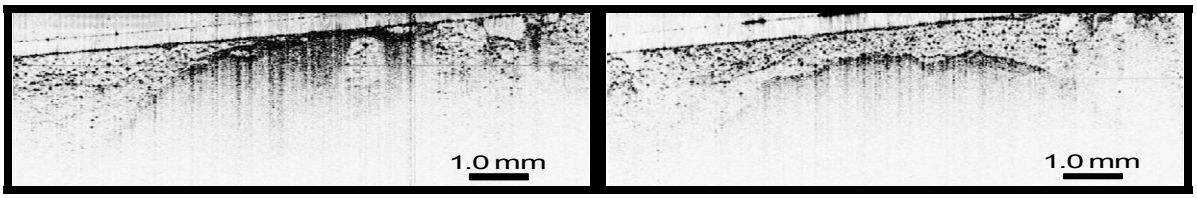

Fig. 8. Intra-operative OCT images taken of an axillary lymph node using the clinical SD-OCT at 1300 nm. The OCT image sizes are 10 x 3 mm. The lymph node can be seen with the capsule (dark layer) and the cortex (lighter layer with small sized scatterers).

3.4 Representative intra-operative optical needle-biopsy data

Intra-operative testing of various optical low-coherence interferometry (LCI) needle probes was performed. These studies consisted of inserting optical needle probes through the surgical margin and into the resected lumpectomy specimens to localize the internal position of the tumor margin (as opposed to examination and imaging of the exterior surgical margin). LCI depth-resolved data was also acquired during needle insertion at multiple points. Needle insertion points and depths were recorded and matched with acquired axial LCI data, for correlations with corresponding histopathological findings. All insertion points and needle insertion trajectories were within a single plane, normal to the surgical margin surface. This plane was identified using surgical inks, and histological sections were taken along with plane for later correlations. A representative schematic of the imaging probe sites, corresponding LCI axial scan data, and corresponding histological tissue section are shown in Fig. 9. Ongoing studies are determining the sensitivity and specificity of this technique, using post-operative histological findings as the gold standard for comparison.

These needle-biopsy feasibility studies have demonstrated the potential for using similar optical needle-biopsy probes to guide the placement of needles for sampling suspicious lesions detected on x-ray mammography, ultrasound, or MRI. These procedures would be performed in more office-based settings, rather than in the operating suite. It is also possible to integrate optical fibers within needle-biopsy devices, to function as a single unit during optical guidance and positioning.

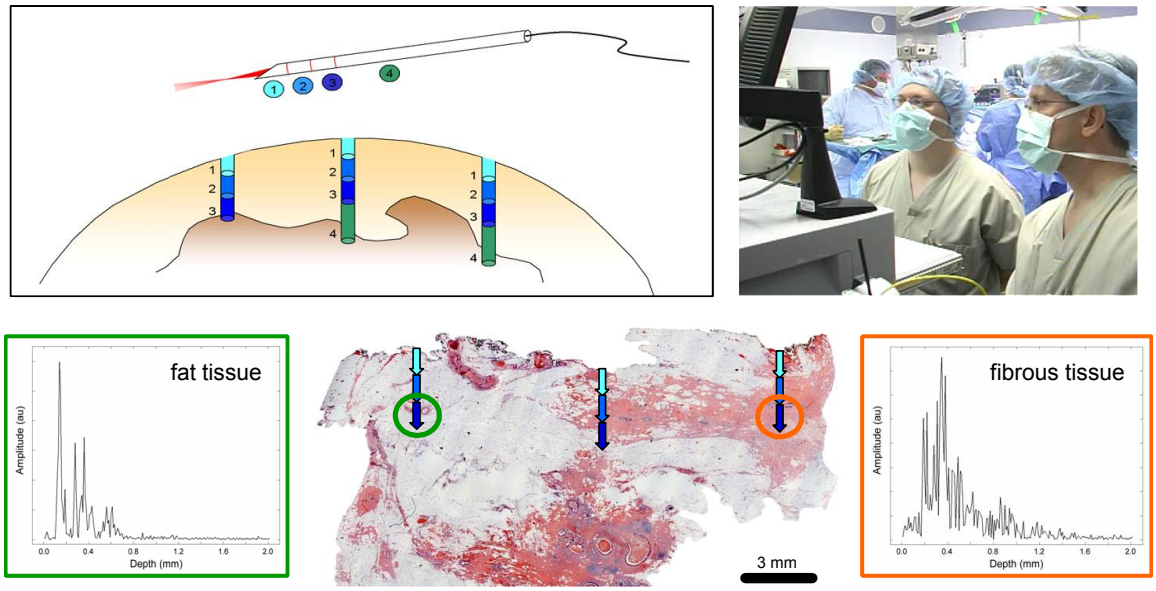

Fig. 9. Schematic of an LCI optical needle probe used in intra-operative studies to localize the tumor margin within a surgically-resected tissue mass. Corresponding LCI axial depth scans are shown, along with positions in the corresponding histological section.

4. DISCUSSION

The initial system validation studies show that although the resolution of the 1300 nm clinical SD-OCT system is not as high as in the 800 nm systems, as expected, there is still remarkable corroboration between the three systems in identifying the tumor margin between the primary tumor and the surrounding adipose tissue. Through these initial studies, the observed penetration depth for breast tissue is approximately 1 mm at 800 nm, and approximately 2 mm at 1300 nm wavelength. These depths, however, are suitable for assessing the exposed surgical margin of the resected tissue to determine whether the surgical margin is either positive or negative for tumor cells. In fact, histopathological sectioning is performed at visually-selected sites on the surgical margin, and margin status is assessed by viewing the 1-2 mm region below the surgical margin surface. Therefore, intra-operative OCT has the potential to visualize the surgical margin at depths and resolutions similar to what is performed in the pathology laboratory.

Upon examination of the pathology reports for the patients whose excised tissue was imaged in the operating room, the average distance between the tumor margin and the surgical margin typically ranged from 10 – 20 mm. Compared to the penetration depth of OCT, it is therefore expected that most of the OCT imaging of the surgical margin would identify normal tissue, and this has been our experience. However, in the U.S., in approximately 10-15% of cases, surgical margins are positive for tumor cells. Our ongoing OCT imaging studies have found approximately 12% of the surgical margins positive, which correlates to the findings identified on the corresponding histopathology following the surgical procedures. These percentages, however, are based on the limited sampling that is performed both by histology and currently by our intra-operative OCT imaging. We anticipate these percentages will increase with the use of high-speed OCT systems coupled with advanced volumetric microscopy [22] and tissue-type classification algorithms [8], which will have the potential for covering larger areas of the surgical margin for the assessment of margin status. Our group is currently investigating this potential.

In these promising preliminary studies, there were cases where areas of higher scattering tissue were observed, which could be clearly differentiated from adipose tissue. Further studies need to be performed to investigate how these areas of higher optical scattering can be classified as being due to the presence of cancer cells, stromal tissue, cauterized tissue, or blood. Initial results suggest that the heterogeneity of the increased scattering is correlated more with the presence of tumor cells, whereas cauterized and stromal tissues appear more homogeneously scattering, and scattering effects from blood can be mitigated by washing and rinsing of the imaging site.

The image data from the lymph nodes also show promising results that warrant further investigation. From the images presented, one can observe distinct morphological differences between the various axillary lymph nodes that have been imaged. Past and ongoing work is investigating optical scattering changes in normal, reactive, and metastatic lymph nodes in a pre-clinical animal model system. The most promising intra-operative imaging results indicate that these morphological structures within the lymph node, particularly the follicles, are within the imaging penetration depth of the OCT system.

The results from the optical needle-biopsy data suggest that tissue type classification can be performed using axial depth-scan data collected using LCI. By coupling these signal analysis and tissue classification algorithms with novel optical needle-biopsy probes, there is the potential to guide the placement of fine-needles and core-needles for tissue biopsy, and for the precise placement of localization wires prior to surgery. We have demonstrated the use of these optical needle probes and tissue classification algorithms in the operating room on freshly resected lumpectomy specimens, used acquired data to determine the location of the interior tumor margin, and classified the tissue types along the needle insertion tracks. Ongoing work is developing optical needle-biopsy probes that would be suitable for *in vivo* human patient use.

5. CONCLUSIONS

These studies have demonstrated the translation of OCT and LCI from laboratory investigations into the clinical environment of the surgical operating room. The portable, real-time, high-resolution imaging capabilities of OCT and LCI enable intra-operative data and image acquisition, with the potential to provide real-time feedback and surgical guidance during procedures. To date, intra-operative results obtained with OCT and LCI have shown strong correspondence with correlating histopathological results, and ongoing studies are determining the sensitivity and specificity of OCT and LCI, compared to histopathological findings, the current post-operative gold standard. These results have the potential to significantly alter the protocols for surgical interventions and procedures by moving the high-resolution optical (microscopic) assessment and diagnostic capabilities out of the pathology laboratory and to the point-of-care, where immediate feedback can be utilized to guide and improve surgical interventional procedures.

REFERENCES

[1] Cancer Facts & Figures 2008. American Cancer Society, 2008.

[2] Breast Cancer Facts & Figures 2007-2008, American Cancer Society, 2008

[3] McLaughlin, S. A., Ochoa-Frongia, L. M., Patil, S. M., Cody, H. S. 3rd, and Sclafani, L. M., "Influence of frozen-section analysis of sentinel lymph node and lumpectomy margin status on reoperation rates in patients undergoing breast-conserving therapy," J. Am. Coll. Surg. 206, 76-82 (2008).

[4] Bakhshandeh, M., Tutuncuoglu, S. O., Fischer, G., and Masood, S., "Use of imprint cytology for assessment of surgical margins in lumpectomy specimens in breast cancer patients," Diagn. Cytopathol. 35, 656-659 (2007).

[5] Clare, S. E., Sener, S. F., Wilkens, W., Goldschmidt, R., Merkel, D., and Winchester, D. J., "Prognostic significance of occult lymph node metastases in node-negative breast cancer," Ann. Surg. Oncol. 4, 447-451 (1997).

[6] Cote, R. J., Peterson, H. F., Chaiwun, B., Gelber, R. D., Goldhirsch, A., Castiglione-Gertsch, M., Gusterson, B., and Neville, A. M., "Role of immunohistochemical detection of lymph-node metastases in management of breast cancer," Lancet 354, 896-900 (1999).

[7] Boppart, S. A., Luo, W., Marks, D. L., and Singletary, K. W., "Optical coherence tomography: feasibility for basic research and image-guided surgery of breast cancer," Breast Cancer Res. Treat. 84, 85-97 (2004).

[8] Zysk, A. M. and Boppart, S. A., "Computational methods for analysis of human breast tumor tissue in optical coherence tomography images," J. Biomed. Opt. 11, 054015 (2006).

[9] Zysk, A. M., Chaney, E. J., and Boppart, S. A., "Refractive index of carcinogen-induced rat mammary tumours," Phys. Med. Biol. 51, 2165-2177 (2006)

[10] Zysk, A. M., Adie, S. G., Armstrong, J. J., Leigh, M. S., Paduch, A., Sampson, D. D., Nguyen, F. T., and Boppart, S. A., "Needle-based refractive index measurement using low coherence interferometry," Opt. Lett. 32, 385-387 (2007).

[11] Hsiung, P. L., Phatak, D. R., Chen, Y., Aguirre, A. D., Fujimoto, J. G., and Connolly, J. L., "Benign and malignant lesions in the human breast depicted with ultrahigh resolution and three-dimensional optical coherence tomography," Radiology 244, 865-874 (2007).
[12] Zysk, A. M., Nguyen, F. T., Oldenburg, A. L., Marks, D. L., and Boppart, S. A., "Optical coherence tomography: a review of clinical development from bench to bedside," J. Biomed. Opt. 12, 051403 (2007).
[13] Nguyen, F. T., Zysk, A. M., Kotynek, J. G., Oliphant, U. J., Bellafiore, F. J., Rowland, K. M., Johnson, P. A., Chaney, E. J., and Boppart, S. A., "Real-time optical coherence tomography for the intraoperative microscopic assessment of surgical margins in breast cancer," Paper 6847-66, SPIE Proceedings, Photonics West – Biomedical Optics, San Jose, CA, January 19-24, 2008
[14] Greene, F. L., Fleming, I. D., Fritz, A. G., Balch, C. M., Haller, D. G., and Morrow, M., eds., American Joint Committee on Cancer Staging Manual. 6th ed., New York, NY: Springer (2002).
[15] Cancer Prevention & Early Detection Facts & Figures, American Cancer Society (2006).
[16] Luo, W., Nguyen, F. T., Zysk, A. M., Ralston, T. S., Brockenbrough, J., Marks, D. L., Oldenburg, A. L, and Boppart, S. A., "Optical biopsy of lymph node morphology using optical coherence tomography," Technol. Cancer Res. Treat. 4, 539-548 (2005).
[17] Nguyen, F. T., Zysk, A. M., Kotynek, J. G., Oliphant, U. J., Brockenbrough, J., Bellafiore, F. J., Rowland, K. M., Johnson, P. A., Chaney, E. J., and Boppart, S. A., "Real-time lymph node assessment using optical coherence tomography for the staging of breast cancer," Paper 6847-107, SPIE Proceedings, Photonics West – Biomedical Optics, San Jose, CA, January 19-24, 2008
[18] Meeske, K. A., Sullivan-Halley, J., Smith, A. W., McTiernan, A., Baumgartner, K. B., Harlan, L. C., and Bernstein, L., "Risk factors for arm lymphedema following breast cancer diagnosis in black women and white women," Breast Cancer Res. Treat., eprint, February 24, 2008.
[19] Zysk, A. M., Marks, D. L., Liu, D. Y., and Boppart, S. A., "Needle-based reflection refractometry of scattering samples using coherence-gated detection," Optics Express 15, 4787-4794 (2007).
[20] Iftimia, N.V., Bouma, B. E., Pitman, M. B., Goldberg, B. Bressner, J., and Tearney, G. J., "A portable, low coherence interferometry based instrument for fine needle aspiration biopsy guidance," Rev. Sci. Instr. 76, 064301 (2005).
[21] Goldberg, B. D., Iftimia, N. V., Bressner, J. E., Pitman, M. B., Halpern, E., Bouma, B. E., Tearney, G. J., "Automated algorithm for differentiation of human breast tissue using low coherence interferometry for fine needle aspiration biopsy guidance," J. Biomed. Opt. 13, 014014 (2008).
[22] Ralston, T. S., Marks, D. L., Carney, P. S., and Boppart, S. A., "Interferometric synthetic aperture microscopy," Nature Physics 3, 129-134 (2007).